Hydrol. Earth Syst. Sci., 21, 1279–1294, 2017
www.hydrol-earth-syst-sci.net/21/1279/2017/
doi:10.5194/hess-21-1279-2017

Hydrology and Earth System Sciences
Open Access
EGU

Extending flood forecasting lead time in a large watershed by coupling WRF QPF with a distributed hydrological model

Ji Li[1], Yangbo Chen[1], Huanyu Wang[1], Jianming Qin[1], Jie Li[2], and Sen Chiao[3]

[1]Department of Water Resources and Environment, Sun Yat-sen University, Guangzhou, 510275, China
[2]Hydrology Bureau, Pearl River Water Resources Commission, Guangzhou, 510370, China
[3]Department of Meteorology and Climate Science, San Jose State University, San Jose, CA 95192, USA

Correspondence to: Yangbo Chen (eescyb@mail.sysu.edu.cn)

Received: 29 September 2016 – Discussion started: 20 October 2016
Accepted: 16 February 2017 – Published: 2 March 2017

Abstract. Long lead time flood forecasting is very important for large watershed flood mitigation as it provides more time for flood warning and emergency responses. The latest numerical weather forecast model could provide 1–15-day quantitative precipitation forecasting products in grid format, and by coupling this product with a distributed hydrological model could produce long lead time watershed flood forecasting products. This paper studied the feasibility of coupling the Liuxihe model with the Weather Research and Forecasting quantitative precipitation forecast (WRF QPF) for large watershed flood forecasting in southern China. The QPF of WRF products has three lead times, including 24, 48 and 72 h, with the grid resolution being 20 km × 20 km. The Liuxihe model is set up with freely downloaded terrain property; the model parameters were previously optimized with rain gauge observed precipitation, and re-optimized with the WRF QPF. Results show that the WRF QPF has bias with the rain gauge precipitation, and a post-processing method is proposed to post-process the WRF QPF products, which improves the flood forecasting capability. With model parameter re-optimization, the model's performance improves also. This suggests that the model parameters be optimized with QPF, not the rain gauge precipitation. With the increasing of lead time, the accuracy of the WRF QPF decreases, as does the flood forecasting capability. Flood forecasting products produced by coupling the Liuxihe model with the WRF QPF provide a good reference for large watershed flood warning due to its long lead time and rational results.

1 Introduction

Watershed flood forecasting is one of the most important non-engineering measures for flood mitigation (Tingsanchali, 2012; Li et al., 2002), and significant progress in watershed flood forecasting has been made in the past decades (Borga et al., 2011; Moreno et al., 2013). Lead time is a key index for watershed flood forecasting, especially for large watersheds (Toth et al., 2000; Han et al., 2007). Only flood forecasting products with a long lead time are useful as they could provide enough time for flood warning and flood emergency responses. In the long practice of flood forecasting, ground-based rain gauge measured precipitation is the main input for flood forecasting models, but as this kind of precipitation is the rainfall falling to the ground already, it has no lead time. This makes watershed flood forecasting have very short lead times (Jasper et al., 2002), and could not satisfy the requirement of flood warning (Shim et al., 2002) in lead time, particularly in large watersheds, thus reducing the value of the flood forecasting products in watershed flood mitigation.

The developed numerical weather prediction models in the past decades could provide a longer lead time quantitative precipitation forecast (QPF) product in grid format. The lead time for the latest weather prediction model could be as long as 1–15 days (Buizza et al., 1999; Ahlgrimm et al., 2016). By coupling the QPF weather prediction model with a flood forecasting model, the flood forecasting lead time could thus be extended. This provides a new way of large watershed flood forecasting (Jasper et al., 2002; Zappa et al., 2010; Giard and Bazile, 2000). Many numer-

ical weather prediction models have been proposed and put into operational use, such as the European Centre Medium-Range Weather Forecasts (ECMWF) Ensemble Prediction System (EPS) (Molteni et al., 1996; Barnier et al., 1995), the Weather Research and Forecasting (WRF) model (Skamarock et al., 2005, 2008; Maussion et al., 2011), the numerical weather forecast model of the Japan Meteorological Agency (Takenaka et al., 2011; Gao and Lian, 2006), the numerical forecast model of the China Meteorological Agency (Li and Chen, 2002), and others.

Watershed flood forecasting relies on a hydrological model for a computation tool, while the precipitation is the model's driving force. The earliest hydrological model is regarded as the Sherman unit graph (Sherman, 1932), which belongs to the category of lumped hydrological models. Many lumped hydrological models have been proposed, such as the Sacramento model (Burnash, 1995), the NAM model (DHI, 2004), and the Xinanjiang model (Zhao, 1977). The lumped hydrological model regards the watershed as a whole hydrological unit; thus, the model parameter is the same over the watershed, but this is not true, particularly for a large watershed. The precipitation the lumped hydrological model uses is averaged over the watershed also. This further increases the model's uncertainty in large watershed flood forecasting as it is well known that the precipitation distribution over the watershed is highly uneven. The QPF produced by numerical weather prediction model forecasts precipitation in grid format, which provides detailed precipitation distribution information over watersheds. This is another advantage of QPF. The lumped hydrological model could not take advantage of gridded WPF products.

The latest development of watershed hydrological models is the distributed hydrological model (Refsgaard, 1997), which divides the watershed into grids, and different grids could have their own precipitation, terrain property and model parameter. Hence a distributed hydrological model is the ideal model for coupling the WRF QPF for watershed flood forecasting. The first proposed distributed hydrological model is the SHE model (Abbott et al., 1986a, b), and now many distributed hydrological models have been proposed, and a few have been used for watershed flood forecasting, such as the SHE model (Abbott et al., 1986a, b), the WATERFLOOD model (Kouwen, 1988), the VIC model (Liang et al., 1994), the WetSpa model (Wang et al., 1997), the Vflo model (Vieux and Vieux, 2002), the WEHY model (Kavvas et al., 2004), and the Liuxihe model (Chen, 2009; Chen et al., 2011).

As the distributed hydrological model calculates the hydrological process at grid scale, so the computation time needed for running the distributed hydrological model is huge even for a small watershed. This limits the model's application in watershed flood forecasting, particularly in a large watershed. Model parameter uncertainty related to the distributed hydrological model also impacted its application. But with the development of a parallel computation algorithm for the distributed hydrological model and its deployment on a supercomputer (Chen et al., 2013), the computation burden is not a great challenge of distributed hydrological modeling anymore. Also, with the development of automatical parameter optimization of the distributed hydrological model in flood forecasting (Madsen, 2003; Shafii and De Smedt, 2009; Xu et al., 2012; Chen et al., 2016), the model parameters could be optimized, and the model's performance could be improved greatly. With these advances, now the distributed hydrological model could be used for large watershed flood forecasting.

In this paper, the WRF QPF is coupled with a distributed hydrological model – the Liuxihe model – for large watershed flood forecasting in southern China. The spatial and temporal resolution of the WRF QPF is at 20 km × 20 km and 1 h, respectively, with three lead times, including 24, 48 and 72 h. The WRF QPF has a similar precipitation pattern to that estimated by rain gauges, but overestimates the averaged watershed precipitation, and the longer the WRF QPF lead time, the higher the precipitation overestimation. Since the WRF QPF has systematic bias compared with rain gauge precipitation, a post-processing method is proposed to post-process the WRF QPF products, which improves the flood forecasting capability. The Liuxihe model is set up with freely downloaded terrain property. The model parameters were previously optimized with rain gauge observed precipitation, and re-optimized with the WRF QPF. With model parameter re-optimization, the model's performance improved. Model parameters should be optimized with QPF, not the rain gauge precipitation. Flood forecasting products produced by coupling the Liuxihe model with the WRF QPF provide a good reference for large watershed flood warning due to their long lead time and rational results.

2 Study area and data

2.1 Study area

The Liujiang River basin (LRB) is selected as the studied area, which is the largest first-order tributary of the Pearl River with a drainage area of 58 270 km^2 (Chen et al., 2017). LRB is in the monsoon area with heavy storms that induced severe flooding in the watershed and caused huge flood damages in the past centuries. Figure 1 is a sketch map of the LRB.

2.2 Rain gauge precipitation and river flow discharge

Precipitation of 68 rain gauges within the watershed in 2011, 2012 and 2013 was collected and used in this study to compare with the WRF QPF. Precipitation data are at 1 h intervals. River discharge near the watershed outlet is collected also for this same period. As this study focuses on watershed flood forecasting, so only the precipitation and river discharge during the flood events are prepared. There is one

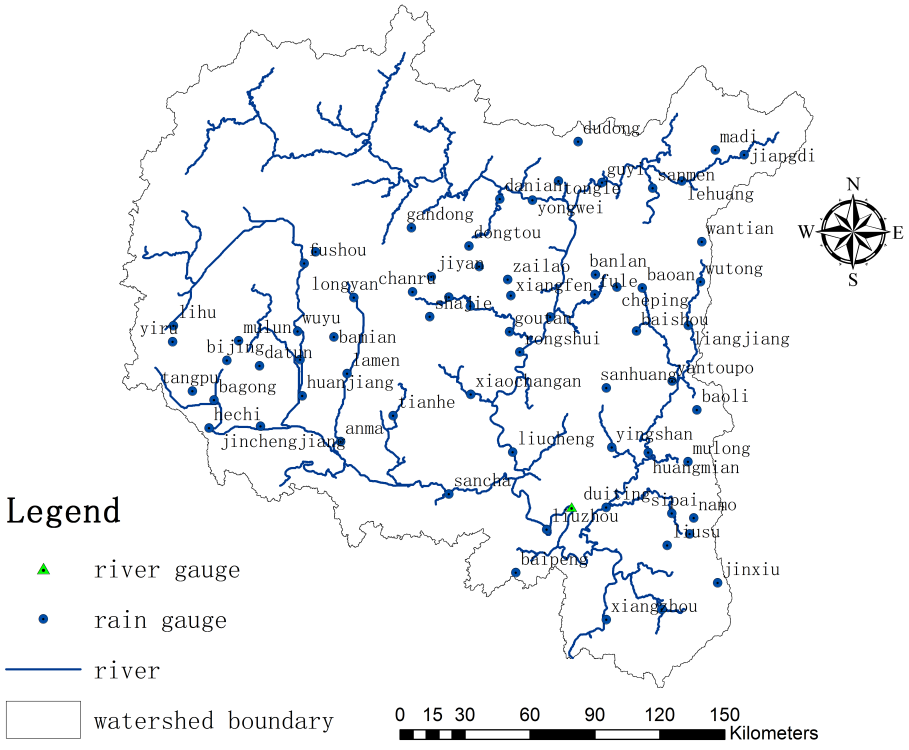

Figure 1. Sketch map of the Liujiang River basin (Chen et al., 2017).

flood event in each year. The flood events are numbered as flood event no. 2011, flood event no. 2012 and flood event no. 2013, respectively.

3 WRF QPFs and their post-processing

3.1 WRF model

All simulations for this study were conducted with the Advanced Research WRF (WRF-ARW) model version 3.4 (Skamarock et al., 2008). The WRF-ARW model is 3-D, non-hydrostatic, and fully compressible, and has the terrain-following sigma coordinate system. The model is considered the next generation's medium-range weather forecasting model, and can simulate different weather processes from cloud scale to synoptic scale, especially at a horizontal resolution of 1–10 km. The model also integrates the advanced numerical methods and data assimilation techniques, a variety of physical process schemes, and multiple nested methods and the capability of being used in different geographical locations. The WRF-ARW model satisfies the needs of scientific research and practical applications for this study.

Prior studies have been shown in quantitative precipitation forecasting by using the WRF-ARW model. For instance, Pennelly et al. (2014) employed the WRF model to predict three precipitation events of Alberta, Canada, and compared the precipitation with the 48 h leading time predicted by the model with rain gauges. The results showed that Kain–Fritsch cumulus parameterization overestimated the value of precipitation invariably. Eiserloh and Chiao (2015) used WRF-ARW with data assimilation to investigate an atmospheric river event over northern California. Maussion et al. (2011) compared the capability of the WRF model in retrieving monthly precipitation and snowfall at three different spatial resolutions, including the 30, 10 and 2 km domains over Tibet. Their results showed that the model was able to recapture monthly precipitation and snowfall. Pan et al. (2012) used two WRF simulation groups between preprocess and post-process in the Heihe River basin, and compared and analyzed the mean bias error, root mean square error and correlation coefficient of the two WRF groups. Huang et al. (2011) found that variations in the microphysical process parameterization schemes had much more influence on precipitation than that of cumulus parameterization schemes, especially for a torrential rain attributed to large-scale forcing that mainly resulted from stratus clouds. Kumar et al. (2001) used the WRF model to study a heavy rain in 2005; their results showed that the WRF model could reproduce the storm event and its dynamical and thermodynamical characteristics. Hong and Lee (2009) conducted a triply nested WRF simulation for convective initiation of a thunderstorm. Givati et al. (2012) predicted the hiemal precipitation events of 2008 and 2009 based on the WRF model in the upstream of the Jordan River, and coupled

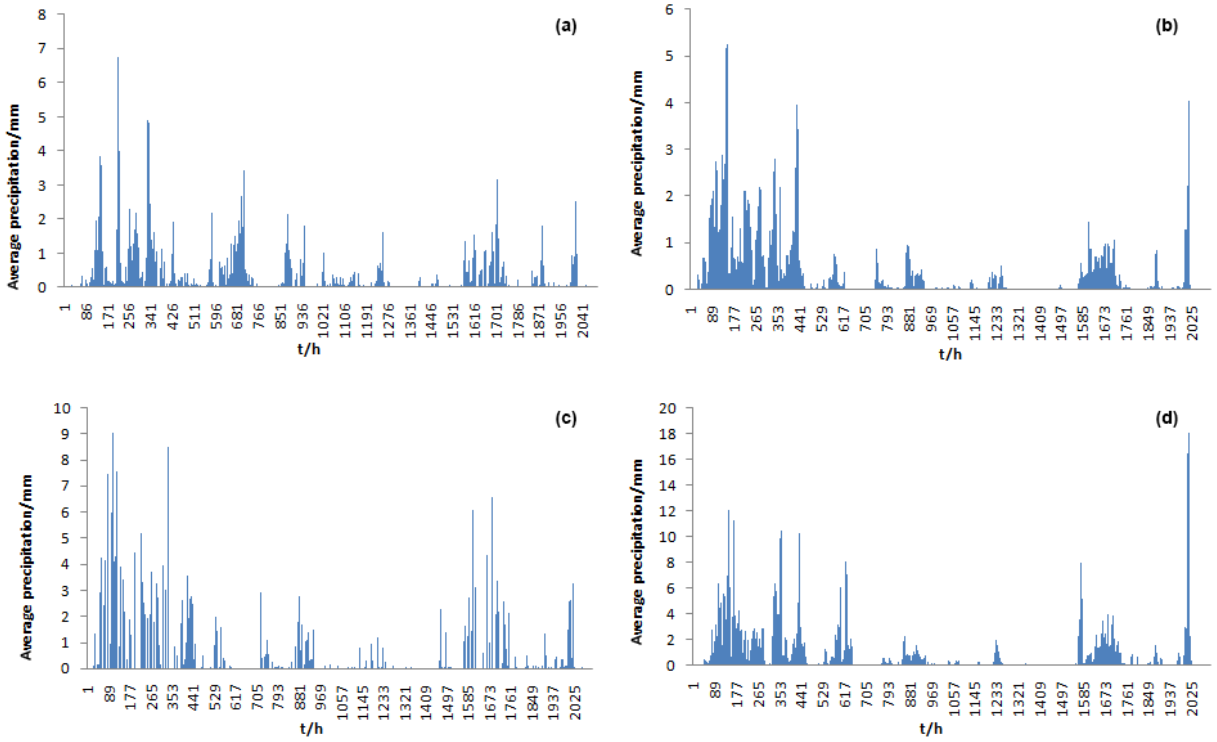

Figure 2. Precipitation pattern comparison of two precipitation products (2011). **(a)** is the average precipitation of rain gauges, **(b)** is the average precipitation of WRF with 24 h lead time, **(c)** is the average precipitation of WRF with 48 h lead time, and **(d)** is the average precipitation of WRF with 72 h lead time.

the WRF model with hydrological model HYMKE to simulate the velocity and discharge of the Jordan River. Sensitivity experiments of WRF microphysical schemes by Niu and Yan (2007) have shown the adequate performance of precipitation predicted associated with region, center location and rainfall intensity. Xu et al. (2007) compared the hiemal continuous precipitation process predicted with the estival results by the WRF model; the results showed that the KF scheme was better than the BM scheme in summer. Hu et al. (2008) found that the parameterization scheme of the WRF model was related to the model resolution, and the parameterization scheme should be selected by the resolution of the WRF model.

3.2 Configuration of WRF for LRB

The WRF-ARW was applied to the LRB following the configurations by Li et al. (2015). More information about the LBR can be found in Li et al. (2015) and Chen et al. (2017). The model domain is centered at 23.8° N, 109.2° W with the Lambert conformal projection. The vertical structure includes 28 levels, with the focus on the lower levels of the troposphere. The initial and time-dependent lateral boundary conditions are supplied from NCEP Global Forecast System (GFS) 3-hourly global analysis at 0.5° horizontal resolution. The model domain has a 20 km grid resolution. The single-moment 3-class microphysics (WSM3) parameterization (Hong and Lim, 2006) is adopted for this study. Kain–Fritsch cumulus parameterization (Kain, 2004) as well as the YSU boundary layer microphysics scheme (Hong and Lim, 2006) are used. Other physics schemes used include the NOAH scheme for the land surface physics (Ek et al., 2003), the Goddard scheme for the shortwave radiation physics (based on Chou and Suarez, 1994), and the Rapid Radiative Transfer Model (RRTM) scheme for the longwave radiation physics (Mlawer et al., 1997).

The spatial and temporal resolution of WRF is at 20 km × 20 km and 1 h, respectively. The entire Liujiang River basin is covered by a total of 156 grid points of the WRF model. The simulated QPF for flood events in years 2011 to 2013 was produced with three different lead times (i.e., 24, 48 and 72 h), respectively. Shown in Figs. 2–4 are the WRF QPF products in 3 different years.

3.3 Evaluation of WRF QPF and rain gauge precipitation

Comparisons of WRF QPF and rain gauge precipitation are performed. From the simulated results, as shown in Figs. 2–4, it appears that the temporal precipitation pattern of both products is similar, although there are some insignificant differences. To make further comparison, the accumulated pre-

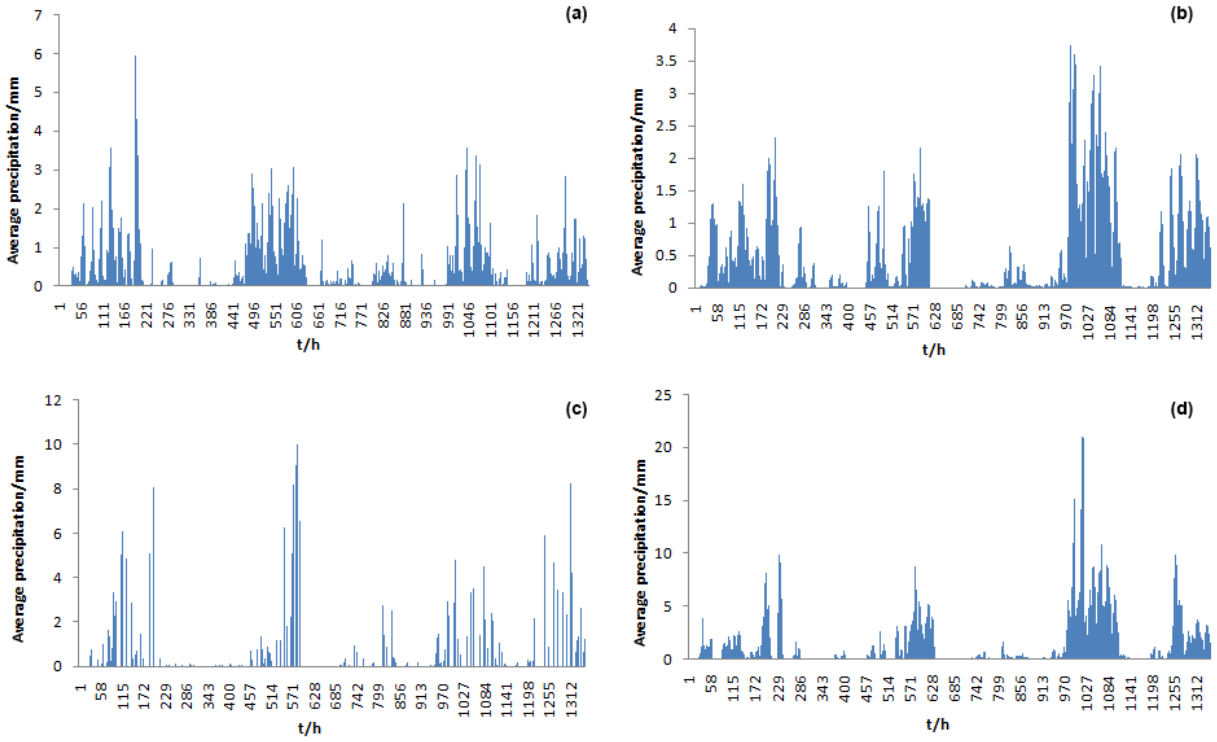

Figure 3. Precipitation pattern comparison of two precipitation products (2012). **(a)** is the average precipitation of rain gauges, **(b)** is the average precipitation of WRF with 24 h lead time, **(c)** is the average precipitation of WRF with 48 h lead time, and **(d)** is the average precipitation of WRF with 72 h lead time.

cipitation of the three flood events averaged over the watershed is calculated and listed in Table 1.

As summarized in Table 1, it could be found that the WRF QPF accumulated precipitation has obvious bias with rain gauge accumulated precipitation. For all three flood events, the WRF QPF accumulated precipitation is higher than that measured by rain gauges. In other words, the WRF QPF overestimates the precipitation. For flood event no. 2011, the overestimated watershed averaged precipitations of the WRF QPF with lead times of 24, 48 and 72 h are 23, 32 and 55 %, respectively. For the flood event no. 2012, they are 16, 37 and 71 %, respectively. They are 50, 73 and 95 %, respectively, from the event no. 2013. The results suggest that the longer the WRF QPF lead time, the higher the chance of overestimation.

Table 1. Precipitation comparison of two products.

Flood event no.	Precipitation products	Average precipitation (mm)	Relative bias %
2011	rain gauges	0.22	
	WRF/24 h	0.27	23
	WRF/48 h	0.29	32
	WRF/72 h	0.34	55
2012	rain gauges	0.38	
	WRF/24 h	0.44	16
	WRF/48 h	0.52	37
	WRF/72 h	0.65	71
2013	rain gauges	0.22	
	WRF/24 h	0.33	50
	WRF/48 h	0.38	73
	WRF/72 h	0.43	95

3.4 WRF QPF statistical calibrations

From the simulated results (cf. Figs. 2–4 and Table 1), the WRF QPF has significant bias compared to rain gauge precipitation. Assuming the rain gauge precipitation is correct, the WRF QPF needs to be further calibrated. In order to do so, the WRF QPF is further post-processed based on the rain gauge precipitation to correct the systematic error of the WRF QPF. The principle of WRF QPF statistical calibrations proposed in this study is to keep the areal averaged event accumulated precipitation from both model and rain gauge products equivalent. In other words, the statistical approach is to nudge the WRF QPF precipitation to rain gauge results.

Based on this principle, the WRF QPF post-processing procedure is summarized as follows.

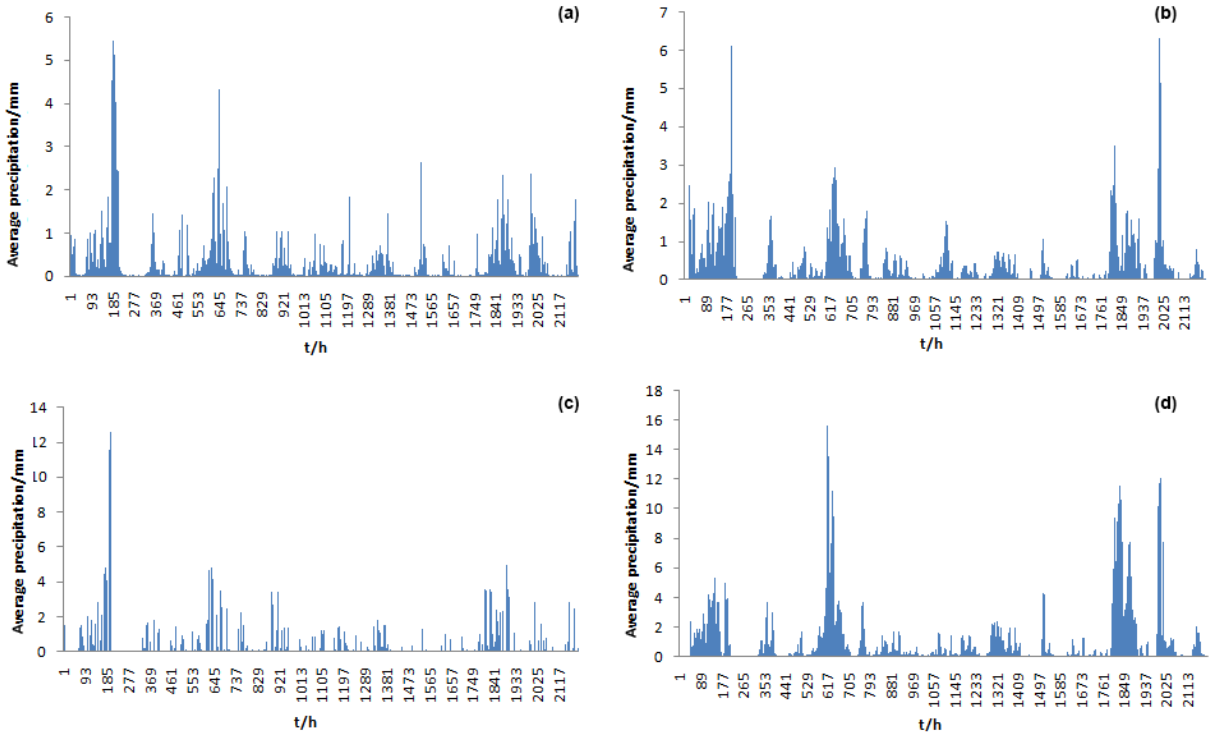

Figure 4. Precipitation pattern comparison of two precipitation products (2013). **(a)** is the average precipitation of rain gauges, **(b)** is the average precipitation of WRF with 24 h lead time, **(c)** is the average precipitation of WRF with 48 h lead time, and **(d)** is the average precipitation of WRF with 72 h lead time.

1. Calculate the areal average precipitation of the WRF QPF for each flood event over the watershed as the following equation:

$$\overline{P}_{\mathrm{WRF}} = \frac{\sum_{i=1}^{N} P_i F_i}{N}, \tag{1}$$

where $\overline{P}_{\mathrm{WRF}}$ is the areal average precipitation of the WRF QPF of one flood event, P_i is the precipitation on WRF grid i, F_i is the surface area of WRF grid i divided by the whole watershed drainage area, and N is the total number of WRF grids.

2. Calculate the areal average precipitation of the rain gauges with the following equation.

$$\overline{P}_2 = \frac{\sum_{j=1}^{M} P_j}{M}, \tag{2}$$

where $\overline{P}_2$ is the areal average precipitation of the rain gauge network, P_j is the precipitation observed by the jth rain gauge, and M is the total number of rain gauges.

3. The precipitation of every WRF QPF grid then could be revised with the following equation.

$$P_i' = P_i \frac{\overline{P}_2}{\overline{P}_{\mathrm{WRF}}}, \tag{3}$$

where P_i' is the revised precipitation of the ith WRF grid.

With the above WRF QPF statistical calibration methods, the WRF QPF of flood events no. 2011, no. 2012 and no. 2013 are post-processed, and will be used to couple with the Liuxihe model for flood simulations.

4 Hydrological model

4.1 Liuxihe model

The Liuxihe model is a physically based fully distributed hydrological model proposed mainly for watershed flood forecasting (Chen, 2009; Chen et al., 2011), and has been used in a few watersheds for flood forecasting (Chen, 2009; Chen et al., 2011, 2013, 2016; Liao et al., 2012a, b; Xu et al., 2012a, b). In the Liuxihe model, runoff components are calculated at grid scale, runoff routes at both grid and watershed scale. Runoff routing is divided into hillslope routing

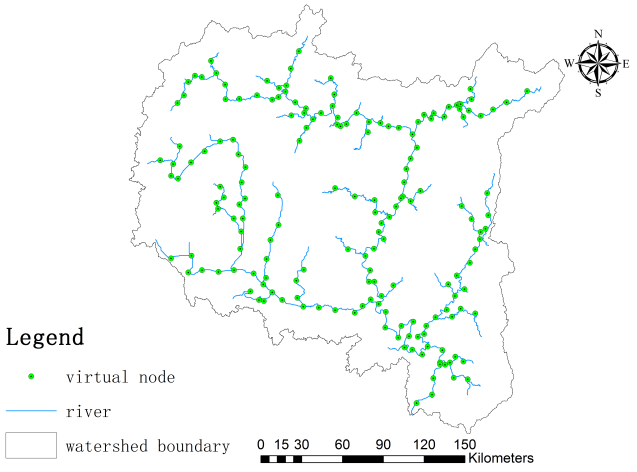

Figure 5. Liuxihe model structure of the LRB (200 m × 200 m resolution, Chen et al., 2017).

and river channel routing by using different computation algorithms. The Liuxihe model proposed an automatic parameter optimization method using the PSO algorithm (Chen et al., 2016), which largely improves the model's performance in watershed flood forecasting. Now the Liuxihe model is deployed on a supercomputer system with parallel computation techniques (Chen et al., 2013) that largely facilitates the model parameter optimization of the Liuxihe model.

Chen et al. (2017) set up the Liuxihe model in the LRB with freely downloaded terrain property data from the website at a spatial resolution of 200 m × 200 m, and optimized model parameters with observed hydrological data. The model was validated by observed flood event data, and the model performance was found to be rational and could be used for real-time flood forecasting. The model only uses rain gauge precipitation, so its flood forecasting lead time is limited. In this study, the Liuxihe model was set up in the LRB and the optimized model parameters were used in this study as the first attempt. Figure 5 shows the model structure.

4.2 Liuxihe model parameter optimization

While the model parameter optimization by Chen et al. (2017) is done by using the rain gauge precipitation, this study uses the WRF QPF as the precipitation input. So the parameters of the Liuxihe model that were set up in the LRB may not be appropriate for coupling the WRF QPF. For this reason, considering the Liuxihe model is a physically based distributed hydrological model, the parameters were optimized again by using the WRF QPF flood event no. 2011. Hence, the WRF QPF is the post-processed one, not the original one. Results of parameter optimization are shown in Fig. 6. Among them, (a) is the objective function evolution result, (b) is the parameter evolution result, and (c) is the simulated flood process by using the optimized model parameters. To compare, the simulated flood process of flood event no. 2011 was also drawn in Fig. 6c.

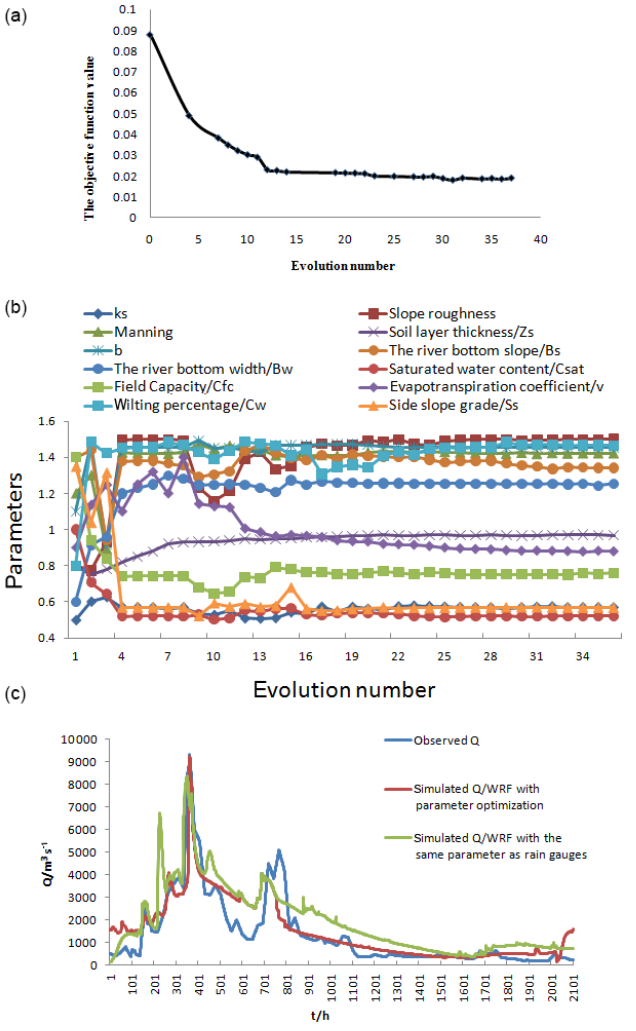

Figure 6. Parameter optimization results of the Liuxihe model for the LRB with WRF QPF.

From the result of Fig. 6c, it may be seen that the optimized model parameters with the WRF QPF improved the flood simulation when compared to the corresponding flood simulation based on gauge precipitation. This means parameter optimization with the WRF QPF is necessary.

4.3 Coupling the WRF QPF with the Liuxihe model for LRB flood forecasting

When the Liuxihe model set up for LRB flood forecasting (Chen et al., 2017) was employed to couple with the WRF QPF, the model spatial resolution remained 200 m × 200 m. As the spatial resolution of the WRF QPF is 20 km × 20 km, the WRF QPF was downscaled to the resolution of 200 m × 200 m by using the nearest downscaling

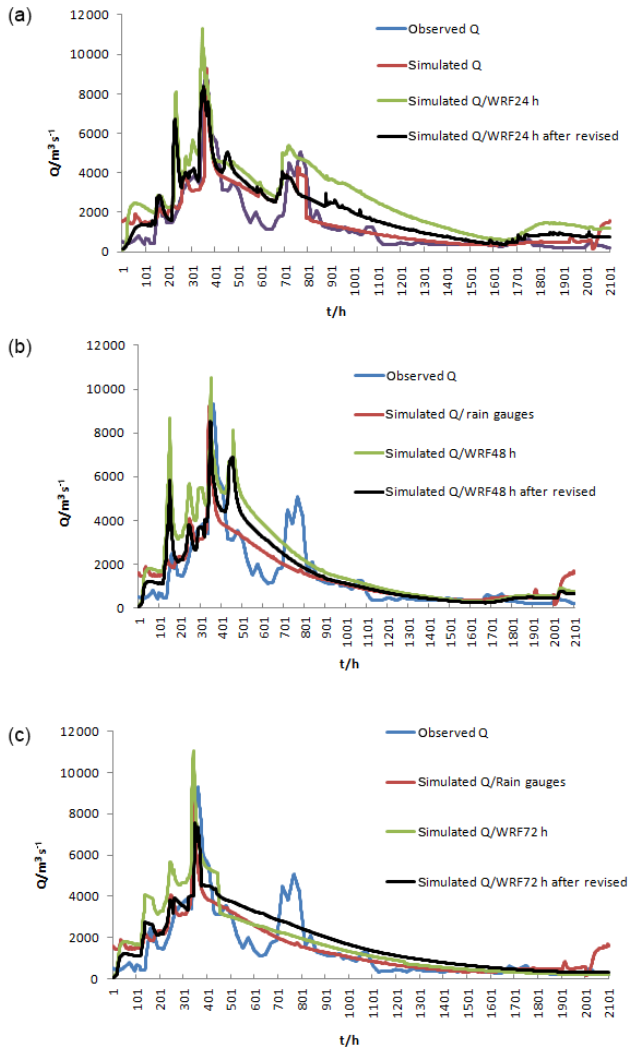

Figure 7. Coupled flood simulation results with the original model parameters (2011). **(a)** is the simulated result with 24 h lead time, **(b)** is the simulated result with 48 h lead time, and **(c)** is the simulated result with 48 h lead time.

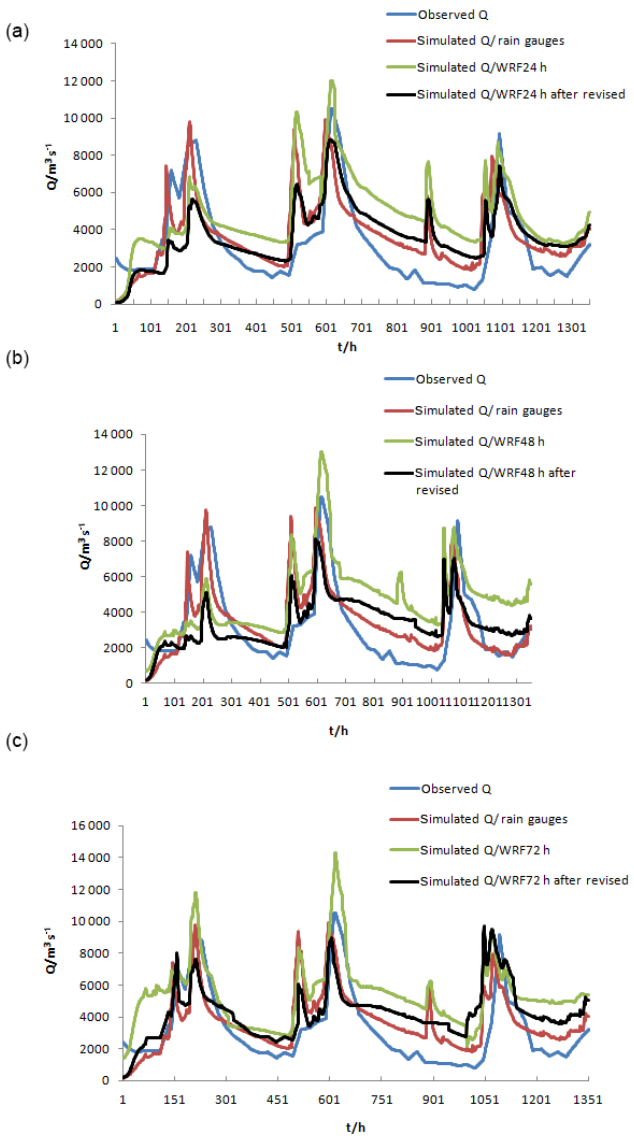

Figure 8. Coupled flood simulation results with the original model parameters (2012). **(a)** is the simulated result with 24 h lead time, **(b)** is the simulated result with 48 h lead time, and **(c)** is the simulated result with 48 h lead time.

method, the same spatial resolution of the flood forecasting model.

5 Results and discussions

5.1 Effects of WRF post-processing

The original WRF QPF and the post-processed QPF were used to couple with the Liuxihe model. In this simulation, the original model parameters that were optimized with the rain gauge precipitation were employed, not the re-optimized model parameters. The simulated results are shown in Figs. 7–9.

From the above results, it could be seen that the simulated flood discharges with the original WRF QPF are much lower than the observed ones. But with the post-processed WRF QPF used, the simulated flood discharge increased and became much closer to the observation. This implies that the flood forecasting capability has been improved by post-processing of the WRF QPF. To further compare the three results, five evaluation indices, including the Nash–Sutcliffe coefficient (C), correlation coefficient (R), process relative error (P), peak flow relative error (E) and water balance coefficient (W), were calculated and listed in Table 2.

From the results of Table 2, it has been found that all five evaluation indices have been improved by coupling the post-processed WRF QPF. For example, for flood event no. 2011 with 24 h lead time, the Nash–Sutcliffe coefficient/C, corre-

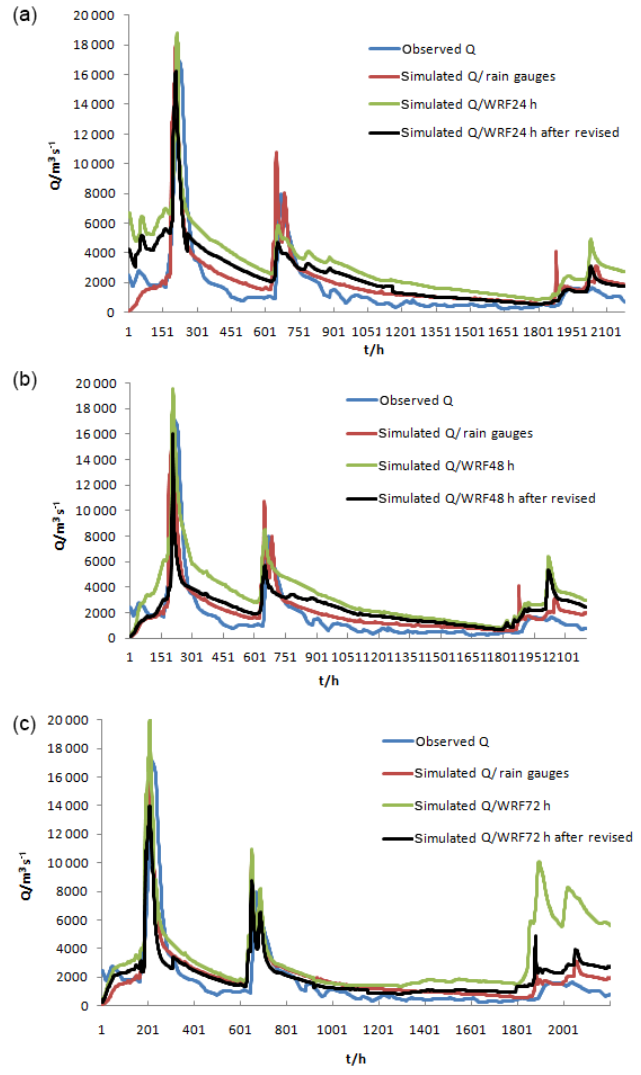

Figure 9. Coupled flood simulation results with the original model parameters (2013). **(a)** is the simulated result with 24 h lead time, **(b)** is the simulated result with 48 h lead time, and **(c)** is the simulated result with 48 h lead time.

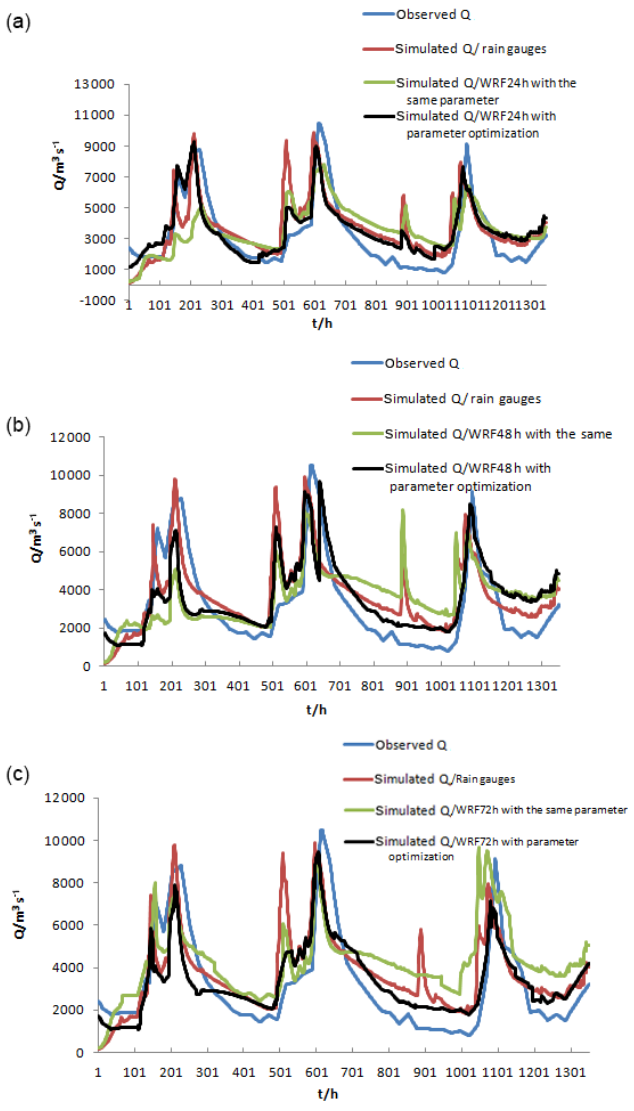

Figure 10. Coupled flood simulation results with the re-optimized model parameters (2012). **(a)** is the simulated result with 24 h lead time, **(b)** is the simulated result with 48 h lead time, and **(c)** is the simulated result with 48 h lead time.

lation coefficient/R, process relative error/P, peak flow relative error/E and coefficient of water balance/W with the original WRF QPF are 0.65, 0.88, 35, 14 % and 1.44, respectively, but those with the post-processed WRF QPF are 0.75, 0.93, 23, 8 % and 1.15, respectively. For flood event no. 2012 with 48 h lead time, the above five evaluation indices with the original WRF QPF are 0.63, 0.75, 48, 12 % and 1.43, respectively, and are 0.75, 0.84, 26, 8 % and 1.32, respectively, with the post-processed WRF QPF. For flood event no. 2013 with 72 h lead time, the above five evaluation indices with the original WRF QPF are 0.44, 0.75, 129, 45 % and 1.66, respectively, and are 0.55, 0.82, 98, 23 % and 1.25, respectively, with the post-processed WRF QPF. It is obvious that with the post-processed WRF QPF, the evaluation indices are improved substantially. These results show that WRF QPF post-processing could improve the flood forecasting capability because the WRF QPF is closer to the observed precipitation after post-processing. So it should be practiced for real-time flood forecasting.

5.2 Results comparison for different model parameters

The model parameters optimized with rain gauge precipitation and the WRF QPF are different, so different parameter values will result in different model performances. To analyze this effect, the flood events no. 2012 and no. 2013 with two different sets of model parameter values are simulated, and are shown in Figs. 10 and 11, respectively. Only the post-processed WRF QPF is coupled in this simulation.

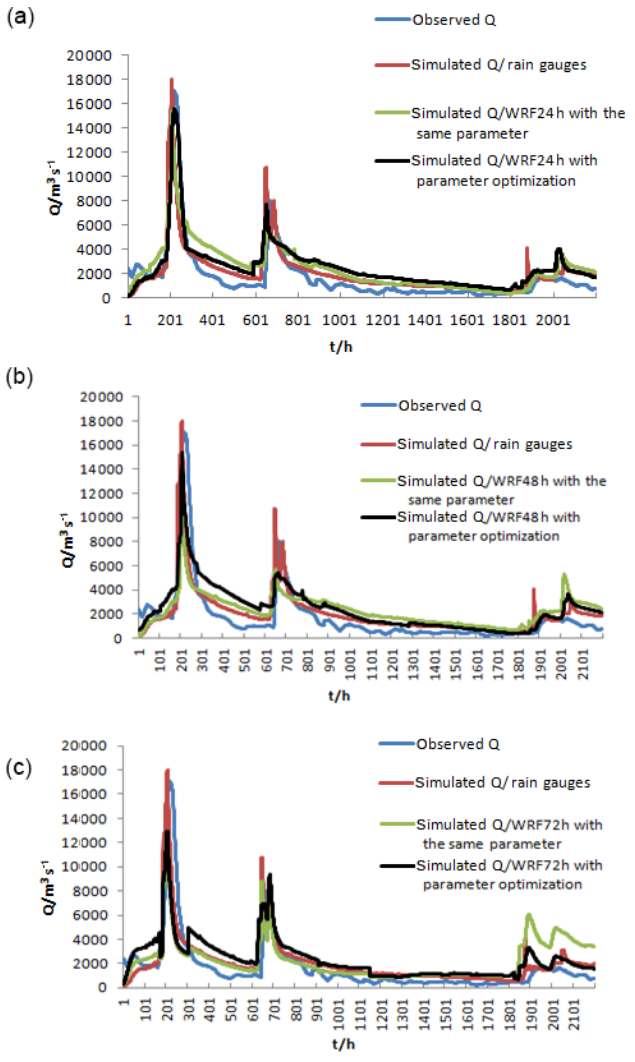

Figure 11. Coupled flood simulation results with re-optimized model parameters (2013). **(a)** is the simulated result with 24 h lead time, **(b)** is the simulated result with 48 h lead time, and **(c)** is the simulated result with 48 h lead time.

From the above figures it may be that the simulated flood results with re-optimized model parameters are better than those simulated with the original model parameters. The simulated flood discharge with the re-optimized model parameters matches the observed discharge. To further compare the two results, five evaluation indices, including the Nash–Sutcliffe coefficient (C), correlation coefficient (R), process relative error (P), peak flow relative error (E) and water balance coefficient (W), are calculated and listed in Table 3.

From the results of Table 3, it is found that the results of flood simulation based on the re-optimized model parameters have better evaluation indices. All evaluation indices for those based on re-optimized model parameters are improved. For example, for flood event no. 2012 with 24 h lead time, the Nash–Sutcliffe coefficient/C, correlation coefficient/R, process relative error/P, peak flow relative error/E and coefficient of water balance/W with the original model parameters are 0.58, 0.82, 35, 12 % and 1.08, respectively, but those with the re-optimized model parameters are 0.74, 0.86, 28, 8 % and 0.95, respectively. For flood event no. 2013 with 48 h lead time, the five indices with the original model parameters are 0.62, 0.86, 22, 13 % and 1.24, respectively, and are 0.68, 0.89, 18, 9 % and 1.06, respectively, for those with re-optimized model parameters. So it could be said that in coupling the WRF QPF with a distributed hydrological model, the model parameters need to be re-optimized with the WRF QPF. This finding implies that the precipitation pattern has an obvious impact on model parameters. It should be considered, and model parameter optimization is a rational way to consider this effect.

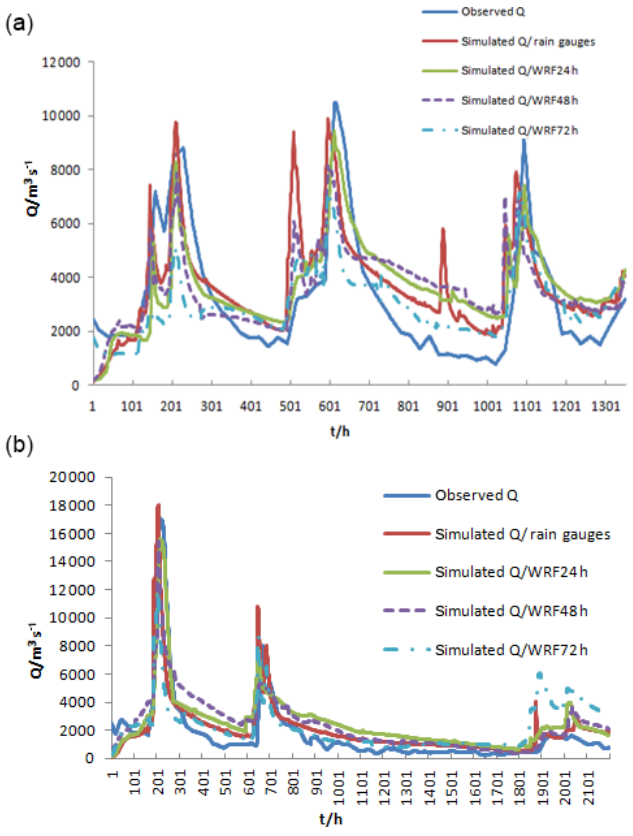

Figure 12. Simulated results with different lead times. **(a)** is the flood simulation results of flood event no. 2012; **(b)** is the flood simulation results of flood event no. 2013.

5.3 Flood simulation accuracy with different lead times

To compare the model performance with different lead times, the flood events with three different lead times are simulated and shown in Fig. 12. The model parameters are the re-optimized ones, and the QPF is the post-processed QPF.

From the results of Fig. 12, it could be seen that the flood simulation result gets worse as the lead time increases; i.e.,

Table 2. Evaluation indices of simulated flood events with the post-processed WRF QPF.

Rain type	Statistical index	Flood event no. 2011	Flood event no. 2012	Flood event no. 2013
WRF/24 h	Nash–Sutcliffe coefficient/C	0.65	0.66	0.65
	Correlation coefficient/R	0.88	0.73	0.83
	Process relative error/P	0.35	0.57	0.19
	Peak flow relative error/E	0.14	0.18	0.25
	The coefficient of water balance/W	1.44	1.35	1.38
WRF/24 h after revised	Nash–Sutcliffe coefficient/C	0.75	0.75	0.75
	Correlation coefficient/R	0.93	0.82	0.85
	Process relative error/P	0.23	0.35	0.11
	Peak flow relative error/E	0.08	0.12	0.16
	The coefficient of water balance/W	1.15	1.08	1.12
WRF/48 h	Nash–Sutcliffe coefficient/C	0.58	0.63	0.5
	Correlation coefficient/R	0.78	0.75	0.8
	Process relative error/P	0.52	0.48	0.34
	Peak flow relative error/E	0.41	0.12	0.24
	The coefficient of water balance/W	1.52	1.43	1.51
WRF/48 h after revised	Nash–Sutcliffe coefficient/C	0.64	0.75	0.62
	Correlation coefficient/R	0.82	0.84	0.86
	Process relative error/P	0.45	0.26	0.22
	Peak flow relative error/E	0.34	0.08	0.13
	The coefficient of water balance/W	1.22	1.32	1.24
WRF/72 h	Nash–Sutcliffe coefficient/C	0.45	0.48	0.44
	Correlation coefficient/R	0.68	0.36	0.75
	Process relative error/P	0.64	0.62	1.29
	Peak flow relative error/E	0.31	0.35	0.45
	The coefficient of water balance/W	1.67	1.54	1.66
WRF/72 h after revised	Nash–Sutcliffe coefficient/C	0.52	0.58	0.55
	Correlation coefficient/R	0.75	0.45	0.82
	Process relative error/P	0.53	0.52	0.98
	Peak flow relative error/E	0.11	0.22	0.23
	The coefficient of water balance/W	1.15	1.14	1.25

the model performance with 24 h lead time is better than that with 48 h lead time, and the model performance with 48 h lead time is better than that with 72 h lead time. The simulated hydrological process with 24 h lead time is very similar to that simulated with rain gauge precipitation. To further compare the results, five evaluation indices, including the Nash–Sutcliffe coefficient (C), correlation coefficient (R), process relative error (P), peak flow relative error (E) and water balance coefficient (W), were calculated and listed in Table 4.

From the results of Table 4, it is found that the simulated flood events with 24 h lead time have the best evaluation indices, and are very close to those simulated with rain gauge precipitation. For flood event no. 2012, the Nash–Sutcliffe coefficient/C, correlation coefficient/R, process relative error/P, peak flow relative error/E and coefficient of water balance/W with the rain gauge are 0.82, 0.89, 20, 5 % and 0.8, respectively, while those with 24 h lead time are 0.74, 0.86, 28, 8 % and 0.95, respectively, those with 48 h lead time are 0.63, 0.84, 48, 12 % and 1.32, respectively, and are 0.56, 0.56, 56, 18 % and 1.54, respectively, for 72 h lead time. For flood event no. 2013, the Nash–Sutcliffe coefficient/C, correlation coefficient/R, process relative error/P, peak flow relative error/E and coefficient of water balance/W with the rain gauge are 0.95, 0.92, 8, 6 % and 1.08, respectively, while those with 24 h lead time are 0.87, 0.87, 9, 12 % and 1.02, respectively, those with 48 h lead time are 0.62, 0.86, 22, 13 % and 1.24, respectively, and are 0.61, 0.87, 75, 17 % and 1.66, respectively, for 72 h lead time. This finding means that the current WRF QPF capability is lead-time-dependent, and with the increasing lead time, the practical value of the WRF QPF gets lower.

Table 3. Evaluation indices of simulated flood events with different model parameters.

Parameter type	Statistical index	Flood event no. 2011	Flood event no. 2012	Flood event no. 2013
Coupling model 24 h/originally optimized model parameters	Nash–Sutcliffe coefficient/C	0.75	0.58	0.75
	Correlation coefficient/R	0.93	0.82	0.85
	Process relative error/P	0.23	0.35	0.11
	Peak flow relative error/E	0.08	0.12	0.16
	The coefficient of water balance/W	1.15	1.08	1.12
Coupling model 24 h/re-optimized model parameters	Nash–Sutcliffe coefficient/C	0.78	0.74	0.87
	Correlation coefficient/R	0.95	0.86	0.87
	Process relative error/P	0.19	0.28	0.09
	Peak flow relative error/E	0.06	0.08	0.12
	The coefficient of water balance/W	1.03	0.95	1.02
Coupling model 48 h/originally optimized model parameters	Nash–Sutcliffe coefficient/C	0.64	0.75	0.62
	Correlation coefficient/R	0.82	0.84	0.86
	Process relative error/P	0.45	0.26	0.22
	Peak flow relative error/E	0.34	0.08	0.13
	The coefficient of water balance/W	1.22	1.32	1.24
Coupling model 48 h/re-optimized model parameters	Nash–Sutcliffe coefficient/C	0.72	0.75	0.68
	Correlation coefficient/R	0.86	0.87	0.89
	Process relative error/P	0.32	0.22	0.18
	Peak flow relative error/E	0.21	0.06	0.09
	The coefficient of water balance/W	1.05	1.12	1.06
Coupling model 72 h/originally optimized model parameters	Nash–Sutcliffe coefficient/C	0.52	0.75	0.55
	Correlation coefficient/R	0.75	0.45	0.82
	Process relative error/P	0.53	0.52	0.98
	Peak flow relative error/E	0.11	0.22	0.23
	The coefficient of water balance/W	1.15	1.14	1.25
Coupling model 72 h/re-optimized model parameters	Nash–Sutcliffe coefficient/C	0.62	0.72	0.61
	Correlation coefficient/R	0.78	0.56	0.87
	Process relative error/P	0.38	0.32	0.75
	Peak flow relative error/E	0.09	0.18	0.17
	The coefficient of water balance/W	1.08	1.02	1.05

6 Conclusion

In this study, the WRF QPF was coupled with a distributed hydrological model – the Liuxihe model – for large watershed flood forecasting, and three lead times of WRF QPF products, including 24, 48 and 72 h, are tested. The WRF QPF post-processing method is proposed and tested, model parameters are re-optimized by using the post-processed WRF QPF, and model performances are compared among various conditions. Based on the results of this study, the following conclusions could be drawn.

1. The quantitative precipitation forecasting produced by the WRF model has a similar pattern to that estimated by rain gauges temporally, but overestimated the averaged watershed precipitation for the event accumulated total precipitation. The longer the WRF QPF lead time, the higher the precipitation overestimation. For flood event no. 2011, the overestimated watershed averaged precipitations of the WRF QPF with lead times of 24, 48 and 72 h are 23, 32 and 55 %, respectively. For flood event no. 2012, these are 16, 37 and 71 %, respectively, while for flood event no. 2013, these are 50, 73 and 95 %, respectively.

2. The WRF QPF has systematic bias compared with rain gauge precipitation, and this bias could be reduced via post-processing. The principle used in this study for WRF QPF post-processing is effective and could improve the flood forecasting capability. For flood event no. 2011 with 24 h lead time, the Nash–Sutcliffe coefficient/C, correlation coefficient/R, process relative error/P, peak flow relative error/E and coefficient of water balance/W with the original WRF QPF are 0.65, 0.88, 35, 14 % and 1.44, respectively, but those with the post-processed WRF QPF are 0.75, 0.93, 23, 8 % and 1.15, respectively. For flood event no. 2012 with

Table 4. Evaluation indices of the simulated flood event with different lead times.

Rain type	Statistical index	Flood event no. 2012	Flood event no. 2013
Rain gauges	Nash–Sutcliffe coefficient/C	0.82	0.95
	Correlation coefficient/R	0.89	0.92
	Process relative error/P	0.2	0.08
	Peak flow relative error/E	0.05	0.06
	The coefficient of water balance/W	0.8	1.08
WRF/24 h	Nash–Sutcliffe coefficient/C	0.74	0.87
	Correlation coefficient/R	0.86	0.87
	Process relative error/P	0.28	0.09
	Peak flow relative error/E	0.08	0.12
	The coefficient of water balance/W	0.95	1.02
WRF/48 h	Nash–Sutcliffe coefficient/C	0.63	0.62
	Correlation coefficient/R	0.84	0.86
	Process relative error/P	0.48	0.22
	Peak flow relative error/E	0.12	0.13
	The coefficient of water balance/W	1.32	1.24
WRF/72 h	Nash–Sutcliffe coefficient/C	0.56	0.61
	Correlation coefficient/R	0.56	0.87
	Process relative error/P	0.56	0.75
	Peak flow relative error/E	0.18	0.17
	The coefficient of water balance/W	1.54	1.66

48 h lead time, the above five evaluation indices with the original WRF QPF are 0.63, 0.75, 48, 12 % and 1.43, respectively, and are 0.75, 0.84, 26, 8 % and 1.32, respectively, with the post-processed WRF QPF. For flood event no. 2013 with 72 h lead time, the above five evaluation indices with the original WRF QPF are 0.44, 0.75, 129, 45 % and 1.66, respectively, and are 0.55, 0.82, 98, 23 % and 1.25, respectively, with the post-processed WRF QPF.

3. Hydrological model parameters optimized with the rain gauge precipitation need to be re-optimized using the post-processed WRF QPF; this improves the model performance significantly. That is, in coupling the distributed hydrological model with QPF for flood forecasting, the model parameters should be optimized with the QPF produced by WRF. For flood event no. 2012 with a 24 h lead time, the Nash–Sutcliffe coefficient/C, correlation coefficient/R, process relative error/P, peak flow relative error/E and coefficient of water balance/W with the original model parameters are 0.58, 0.82, 35, 12 % and 1.08, respectively, but those with the re-optimized model parameters are 0.74, 0.86, 28, 8 % and 0.95, respectively. For flood event no. 2013 with a 48 h lead time, the five indices with the original model parameters are 0.62, 0.86, 22, 13 % and 1.24, respectively, and are 0.68, 0.89, 18, 9 % and 1.06, respectively, for those with re-optimized model parameters.

4. The simulated floods by coupling WRF QPF with the distributed hydrological model are rational and could benefit the flood management communities due to their longer lead times for flood warning. They provide a good reference for large watershed flood warning. But with the lead time getting longer, the flood forecasting accuracy is getting lower. For flood event no. 2012, the Nash–Sutcliffe coefficient/C, correlation coefficient/R, process relative error/P, peak flow relative error/E and coefficient of water balance/W with the rain gauge are 0.82, 0.89, 20, 5 % and 0.8, respectively, while those with a 24 h lead time are 0.74, 0.86, 28, 8 % and 0.95, respectively, those with a 48 h lead time are 0.63, 0.84, 48, 12 % and 1.32, respectively, and are 0.56, 0.56, 56, 18 % and 1.54, respectively, for a 72 h lead time. For flood event no. 2013, the Nash–Sutcliffe coefficient/C, correlation coefficient/R, process relative error/P, peak flow relative error/E and coefficient of water balance/W with the rain gauge are 0.95, 0.92, 8, 6 % and 1.08, respectively, while those with a 24 h lead time are 0.87, 0.87, 9, 12 % and 1.02, respectively, those with a 48 h lead time are 0.62, 0.86, 22, 13 %, and 1.24, respectively, and are 0.61, 0.87, 75, 17 % and 1.66, respectively, for a 72 h lead time.

7 Data availability

The rain gauge precipitation and river flow discharge data were provided by the Bureau of Hydrology, Pearl River Water Resources Commission, China, exclusively used for this study. The WRF QPF results were provided by Yuan Li, and have been published and cited in this paper (Li et al., 2015). The Liuxihe model used in this study is provided by Yangbo Chen, and has been published and cited in this paper (Chen et al., 2017).

Competing interests. The authors declare that they have no conflict of interest.

Acknowledgements. This study is supported by the Special Research Grant for the Water Resources Industry (funding no. 201301070), the National Science Foundation of China (funding no. 50479033), and the Basic Research Grant for Universities of the Ministry of Education of China (funding no. 13lgjc01).

Edited by: Y. Chen
Reviewed by: M. L. Kavvas and one anonymous referee

References

Abbott, M. B., Bathurst, J. C., Cunge, J. A., O'Connell, P. E., and Rasmussen, J.: An Introduction to the European Hydrologic System-System Hydrologue Europeen, "SHE", a: History and Philosophy of a Physically-based, Distributed Modelling System, J. Hydrol., 87, 45–59, 1986a.

Abbott, M. B., Bathurst, J. C., Cunge, J. A., O'Connell, P. E., and Rasmussen, J.: An Introduction to the European Hydrologic System-System Hydrologue Europeen, "SHE", b: Structure of a Physically based, distributed modeling System, J. Hydrol., 87, 61–77, 1986b.

Ahlgrimm, M., Forbes, R. M., Morcrette, J.-J., and Neggers, R. A.: ARM's Impact on Numerical Weather Prediction at ECMWF, Meteorol. Monogr., 57, 28.1–28.13, 2016.

Barnier, B., Siefridt, L., and Marchesiello, P.: Thermal forcing for a global ocean circulation model using a three-year climatology of ECMWF analyses, J. Mar. Syst., 6, 363–380, 1995.

Borga, M., Borga, E. N., Anagnostou, E. N., Bloschl, G., and Creutine, J. D.: Flash flood forecasting, warning and risk management: the HYDRATE project, Environ. Sci. Policy, 14, 834–844, 2011.

Buizza, R., Miller, M., and Palmer, T. N.: Stochastic representation of model uncertainties in the ECMWF Ensemble Prediction System, Q. J. Roy. Meteorol. Soc., 125, 2887–2908, 1999.

Burnash, R. J.: The NWS river forecast system-catchment modeling, in: Computer models of watershed hydrology, edited by: Singh, V. P., Water Resource Publications, Littleton, Colorado, 311–366, 1995.

Chen, Y.: Liuxihe Model, China Science and Technology Press, Peking, China, September 2009.

Chen, Y., Ren, Q. W., Huang, F. H., Xu, H. J., and Cluckie, I.: Liuxihe Model and its modeling to river basin flood, J. Hydrol. Eng., 16, 33–50, 2011.

Chen, Y., Dong, Y., and Zhang, P. C.: Study on the method of flood forecasting of small and medium sized catchment, Proceeding of the 2013 meeting of the Chinese Society of Hydraulic Engineering, 26–28 November 2013, Guangzhou, China, 1001–1008, 2013.

Chen, Y., Li, J., and Xu, H.: Improving flood forecasting capability of physically based distributed hydrological models by parameter optimization, Hydrol. Earth Syst. Sci., 20, 375–392, doi:10.5194/hess-20-375-2016, 2016.

Chen, Y., Li, J., Wang, H., Qin, J., and Dong, L.: Large-watershed flood forecasting with high-resolution distributed hydrological model, Hydrol. Earth Syst. Sci., 21, 735–749, doi:10.5194/hess-21-735-2017, 2017.

Chou, M. D. and Suarez, M. J.: An efficient thermal infrared radiation parameterization for use in general circulation models, NASA Tech. Memo 104606, NASA, 1–92, 1994.

DHI – Danish Hydraulic Institute: MIKE11: A Modeling System for Rivers and Channels User-guide Manual, DHI, Horsholm, Denmark, 2004.

Eiserloh, A. J. and Chiao, S.: Modeling studies of landfalling atmospheric rivers and orographic precipitation over northern California, Meteorol. Atmos. Phys., 127, 1–16, 2015.

Ek, M. B., Mitchell, K. E., Lin, Y., Rogers, E., Grunmann, P., Koren, V., Gayno, G., and Tarpley, J. D.: Implementation of Noah land surface model advances in the National Centers for Environmental Prediction operational mesoscale Eta model, J. Geophys. Res.- Atmos., 108, 1–16, doi:10.1029/2002JD003296, 2003.

Gao, S. and Lian, Q.: Inspection and evaluation numerical forecast product of Japan in precipitation forecasting in Dandong, Meteorology, 6, 79–83, 2006.

Giard, D. and Bazile, E.: Implementation of a New Assimilation Scheme for Soil and Surface Variables in a Global NWP Model, Mon. Weather Rev., 128, 997–1015, 2000.

Givati, A., Barry, L., Liu, Y., and Rimmer, A.: Using the WRF Model in an Operational Stream flow Forecast System for the Jordan River, J. Appl. Meteorol. Clim., 51, 285–299, doi:10.1175/JAMC-D-11-082.1, 2012.

Han, D. W., Kwong, T., and Li, S.: Uncertainties in real-time flood forecasting with neural networks, Hydrol. Process., 21, 223–228, 2007.

Hong, S. and Lim, J.: The WRF Single-Moment 6-Class Microphysics Scheme (WSM6), J. Korean Meteorol. Soc., 42, 129–151, 2006.

Hong, S.-Y. and Lee, J.-W.: Assessment of the WRF model in reproducing a flash-flood heavy rainfall event over Korea, Atmos. Res., 93, 818–831, 2009.

Hu, X., Tao, J., Zheng, F., Wang, N., Zhang, T., Liu, S., and Shang, D.: Synopsis the parameterized scheme of physical process of WRF, Gansu Sci. Technol., 24, 73–75, 2008.

Huang, H., Chen, C., and Zhu, W.: Impacts of Different Cloud Microphysical Processes and Horizontal Resolutions of WRF Model on Precipitation on Forecast Effect, Meteorol. Sci. Technol., 39, 529–536, 2011.

Jasper, K., Gurtz, J., and Lang, H.: Advanced flood forecasting in Alpine watersheds by coupling meteorological observations and

forecasts with a distributed hydrological model, J. Hydrol., 267, 40–52, 2002.

Kain, J. S.: The Kain–Fritsch convective parameterization: An update, J. Appl. Meteorol. Clim., 43, 170–181, 2004.

Kavvas, M., Chen, Z., Dogrul, C., Yoon, J., Ohara, N., Liang, L., Aksoy, H., Anderson, M., Yoshitani, J., Fukami, K., and Matsuura, T.: Watershed Environmental Hydrology (WEHY) Model Based on Upscaled Conservation Equations: Hydrologic Module, J. Hydrol. Eng., 6, 450–464, 2004.

Kouwen, N.: WATFLOOD: A Micro-Computer based Flood Forecasting System based on Real-Time Weather Radar, Can. Water Resour. J., 13, 62–77, 1988.

Kumar, A., Dudhia, J., Rotunno, R., Niyogi, D., and Mohanty, U. C.: Analysis of the 26 July 2005 heavy rain event over Mumbai, India using the Weather Research and Forecasting (WRF) model, Q. J. Roy. Meteorol. Soc., 34, 1897–1910, 2001.

Li, H., Liu, H., Yuan, X., and Liu, S.: The recognition theory of ANN and its application in flood forecasting, Shui Li Xue Bao, 06, 15–19, 2002.

Li, Y., Lu, G. H., Wu, Z. Y., and Shi, J.: Study of a dynamic downscaling scheme for quantitative precipitation forecasting, Remote Sensing and GIS for Hydrology and Water Resources, Proc. IAHS, 368, 108–113, doi:10.5194/piahs-368-108-2015, 2015.

Li, Z. H. and Chen, D.: The development and application of the operational ensemble prediction system at national meteorological center, J. Appl. Meteorol. Sci., 13, 1–15, 2002.

Liang, X., Lettenmaier, D. P., Wood, E. F., and Burges, S. J.: A simple hydrologically based model of land surface water and energy fluxes for general circulation models, J. Geophys. Res., 99, 14415–14428, 1994.

Liao, Z. H., Chen, Y., Xu. H. J., Yan, W. L., and Ren, Q. W.: Parameter Sensitivity Analysis of the Liuxihe Model Based on E-FAST Algorithm, Trop. Geogr., 32, 606–612, 2012a.

Liao, Z. H., Chen, Y., Xu, H. J., and He, J. X.: Study of Liuxihe Model for flood forecast of Tiantoushui Watershed, Yangtze River, 43, 12–16, 2012b.

Madsen, H.: Parameter estimation in distributed hydrological catchment modelling using automatic calibration with multiple objectives, Adv. Water Resour., 26, 205–216, 2003.

Maussion, F., Scherer, D., Finkelnburg, R., Richters, J., Yang, W., and Yao, T.: WRF simulation of a precipitation event over the Tibetan Plateau, China – an assessment using remote sensing and ground Observations, Hydrol. Earth Syst. Sci., 15, 1795–1817, doi:10.5194/hess-15-1795-2011, 2011.

Mlawer, E. J., Taubman, S. J., Brown, P. D., Iacono, M. J., and Clough, S. A.: Radiative transfer for inhomogeneous atmospheres: RRTM, a validated correlated-*k* model for the longwave, J. Geophys. Res.-Atmos., 102, 16663–16682, doi:10.1029/97JD00237, 1997.

Molteni, F., Buizza, R., Palmer, T. N., and Petroliagi, T.: The ECMWF Ensemble Prediction System: Methodology and validation, Q. J. Roy. Meteorol. Soc., 122, 73–119, 1996.

Moreno, H. A., Vivoni, E. R., and Gochis, D. J.: Limits to Flood Forecasting in the Colorado Front Range for Two Summer Convection Periods Using Radar Nowcasting and a Distributed Hydrologic Model, J. Hydrometeorol., 14, 1075–1097, 2013.

Niu, J. and Yan, Z.: The impact on the heavy rain forecast based on physical process of WRF, Sci. Technol. Inform., 23, 42–45, doi:10.3969/j.issn.1001-9960.2007.23.011, 2007.

Pan, X. D., Li, X., Ran, Y. H., and Liu, C.: Impact of Underlying Surface Information on WRF Model in Heihe River Basin, Platea Umeteorol., 31, 657–667, 2012.

Pennelly, C., Reuter, G., and Flesch, T.: Verification of the WRF model for simulating heavy precipitation in Alberta, Atmos. Res., 135–136, 172–192, 2014.

Refsgaard, J. C.: Parameterisation, calibration and validation of distributed hydrological models, J. Hydrol., 198, 69–97, 1997.

Shafii, M. and De Smedt, F.: Multi-objective calibration of a distributed hydrological model (WetSpa) using a genetic algorithm, Hydrol. Earth Syst. Sci., 13, 2137–2149, doi:10.5194/hess-13-2137-2009, 2009.

Sherman, L. K.: Streamflow from rainfall by the unit-graph method, Eng. News-Rec., 108, 501–505, 1932.

Shim, K.-C., Darrell, G. F., Asce, M., and John, W. L.: Spatial Decision Support System for Integrated River Basin Flood Control, J. Water Resour. Pl. Manage., 128, 190–201, doi:10.1061/(ASCE)0733-9496(2002)128:3(190), 2002.

Skamarock, W. C., Klemp, J. B., Dudhia, J., Gill, D. O., Barker, D. M., Wang, W., and Powers, J. G.: A Description of the Advanced Research WRF Version 2, NCAR Technical Note, NCAR/TN-468, STR, National Center For Atmospheric Research, Boulder, CO, Mesoscale and Microscale Meteorology Div., Denver, Colorado, USA, 2005.

Skamarock, W. C., Klemp J. B., Dudhia, J., Gill, D. O., Barker, D. M., Duda, G., Huang, X., Wang, W., and Powers, J. G.: A Description of the Advanced Research WRF Version 3, NCAR Technical Note, NCAR/TN-468, STR, National Center For Atmospheric Research, Boulder, CO, Mesoscale and Microscale Meteorology Div., Denver, Colorado, USA, 2008.

Takenaka, H., Nakajima, T. Y., Higurashi, A., Higuchi, A., Takamura, T., Pinker, R. T., and Nakajima, T.: Estimation of solar radiation using a neural network based on radiative transfer, J. Geophys. Res., 116, D08215, doi:10.1029/2009JD013337, 2011.

Tingsanchali, T.: Urban flood disaster management, Procedia Eng., 32, 25–37, 2012.

Toth, E., Brath, A., and Montanari, A.: Comparison of short-term rainfall prediction models for real-time flood forecasting, J. Hydrol., 239, 132–147, 2000.

Vieux, B. E. and Vieux, J. E.: VfloTM: A Real-time Distributed Hydrologic Model, in: Proceedings of the 2nd Federal Interagency Hydrologic Modeling Conference, 28 July–1 August 2002, Las Vegas, Nevada, 2002.

Wang, Z., Batelaan, O., and De Smedt, F.: A distributed model for water and energy transfer between soil, plants and atmosphere (WetSpa), J. Phys. Chem. Earth, 21, 189–193, 1997.

Xu, G. Q., Liang, X. D., Yu, H., Huang, L. P., and Xue, J. S.: Precipitation Simulation Using Different Cloud-Precipitation Schemes for a Landfall Typhoon, Platea Umeteorol., 26, 891–900, 2007.

Xu, H. J., Chen, Y., Zeng, B. Q., He, J. X., and Liao, Z. H.: Application of SCE-UA Algorithm to Parameter Optimization of Liuxihe Model, Trop. Geogr., 1, 32–37, 2012a.

Xu, H. J., Chen, Y., Li, Z. Y., and He, J. X.: Analysis on parameter sensitivity of distributed hydrological model based on LH-OAT Method, Yangtze River, 43, 19–23, 2012b.

Zappa, M., Beven, K. J., Bruen, M., Cofino, A. S., Kok, E. M., Nurmi, P., Orfila, B., Roulin, E., Schroter, K., Seed, A., Szturc, J., Vehvilainen, B., Germann, U., and Rossa, A.: Propagation of uncertainty from observing systems and NWP into hydrological models: COST-731 Working Group 2, Atmos. Sci. Lett., 11, 83–91, 2010.

Zhao, R. J.: Flood forecasting method for humid regions of China, East China College of Hydraulic Engineering, Nanjing, China, 1977.